

**2011 NDIA GROUND VEHICLE SYSTEMS ENGINEERING AND TECHNOLOGY
SYMPOSIUM
MODELING & SIMULATION, TESTING AND VALIDATION (MSTV) MINI-SYMPOSIUM
AUGUST 9-11 DEARBORN, MICHIGAN**

**SAMPLING-BASED RBDO USING STOCHASTIC SENSITIVITY AND
DYNAMIC KRIGING FOR BROADER ARMY APPLICATIONS**

**K.K. Choi, Ikjin Lee, Liang
Zhao, and Yoojeong Noh**
Department of Mechanical and
Industrial Engineering
The University of Iowa
Iowa City, IA

**David Lamb
and David Gorsich**
US Army TARDEC
Warren, MI

ABSTRACT

The University of Iowa has successfully developed Reliability-Based Design Optimization (RBDO) method and software tools by utilizing the sensitivity analysis of the fatigue life; and applied RBDO to Army ground vehicle components to obtain reliable optimum designs with significantly reduced weight and improved fatigue life. However, this method cannot be applied to broader Army application problems due to lack of sensitivity analysis in many application areas. Thus, for broader Army applications, a sampling-based RBDO method using surrogate model has been developed recently. The Dynamic Kriging (DKG) method is used to generate surrogate models, and a stochastic sensitivity analysis is used to compute the sensitivities of probabilistic constraints with respect to independent and correlated random variables. Once the DKG method accurately approximates the responses, there is no further approximation in the estimation of the probabilistic constraints and stochastic sensitivities, and thus the sampling-based RBDO can yield very accurate optimum design. For computational efficiency of the sampling-based RBDO method for large-scale engineering problems, a parallel computing is proposed. Numerical examples verify that the proposed sampling-based RBDO finds the optimum designs very accurately and efficiently.

1. INTRODUCTION

Significant advances in computing power provide design engineers and decision-makers opportunities to explore many more alternative simulation-based designs than they could do with hardware prototypes. However, when the deterministic optimization method is used, the optimum designs are pushed to the limits of the design constraint boundaries, leaving very little or no room for physical input uncertainties such as manufacturing dimensional variabilities, material property variabilities, simulation model uncertainties, and operational load variabilities, as shown in Fig. 1. Thus, the deterministic optimum designs obtained without consideration of these input uncertainties are unreliable. Due to the extensive efforts of engineering disciplines over last three decades, design guidelines and/or standards have been modified to incorporate the concept of uncertainty in the early design stage. Techniques have been explored to incorporate uncertainty analysis at an affordable computational cost and, more recently, to carry out design

optimization with the additional requirement of reliability, which is referred to as reliability-based design optimization (RBDO) [1-10].

For the most probable point (MPP) based RBDO, to alleviate the slow convergence of the reliability index approach (RIA), the performance measure approach (PMA) is developed by carrying out the inverse reliability analysis [5-7] for a robust and efficient RBDO computational process. For the inverse reliability analysis, the enhanced hybrid mean value (HMV+) method has been developed [11,12] to improve the computational efficiency and stability for highly nonlinear and non-monotonic performance functions [13,14]. The interpolation method of the HMV+ has been further improved by using the angle-based parameter and has been integrated in the enriched performance measure approach (PMA+) for RBDO [15,16]. The PMA+ method has been demonstrated to be very robust and efficient [17].

The reliability analysis using FORM is inaccurate if the performance function is highly nonlinear and multi-dimensional. Although the reliability analysis using SORM may be accurate, it is not easy to use since SORM requires the second-order sensitivities. To overcome these drawbacks by maintaining the efficiency of FORM and the accuracy of SORM, the most probable point based dimension reduction method (MPP-based DRM) has been developed by the Iowa team [18-20].

For the input joint CDF model, the copula, which links between the joint CDF and marginal CDFs, is used [21,22]. Since the copula requires only the marginal CDFs and correlation parameters to generate the joint CDF, the joint CDF can be obtained for practical industrial applications. To identify the correct joint CDF type using the limited test data, it is necessary to find a right copula that best describes the paired sampled data. The two-step weight-based Bayesian method, which selects a right copula among candidate copulas based on the test data, is used [23].

other random input variables is required to carry out the inverse reliability analysis using HVM+ and design optimization using PMA+ [14,15].

The propagation of the input uncertainty into the structural fatigue life is complicate and thus a challenging task to integrate the multidisciplinary software systems and develop the RBDO process for durability optimization. The Iowa research team has developed the *DRAW software system* [26], which computes the transient dynamic stress and strain histories and fatigue life of mechanical components [27,28]. In addition, the *DSO software system* that computes the design sensitivity of various performance measures, including fatigue life, has been implemented by using the continuum design sensitivity theories that the Iowa team has developed [29-31]. These two software systems are integrated with the commercial CAD-Pro/E [32], FEA-NEiNastran [33], multibody dynamics code DADS [34], and design optimization code DOT [35], along with the *PMA+ RBDO software system* that was developed by the Iowa-TARDEC collaborative research team (see Fig. 1). This integrated software system was successfully applied to obtain reliable optimum designs with significantly reduced weight and improved fatigue life of U.S. Army High Mobility Trailer (HMT) drawbar [36], Stryker A-arm [37] shown in Fig. 1, and HMMWV A-arm [38] components.

The system-level durability RBDO of the Army vehicle is a very compute-intensive process because it covers a number of critical vehicle components; with each component consisting of an FEA model possibly up-to hundreds of thousands of DOF. Thus, it could take very long computational time to carry out the vehicle system-level durability RBDO on a single computer processor. The Iowa and TARDEC research team initiated development and testing of a *parallelized DRAW-DSO-RBDO integrated software system* on the TARDEC High Performance Computing (HPC) as shown in Fig. 2. The objective is to obtain a vehicle system-level reliability-based optimum design for weight reduction and durability of all critical components of the Army ground vehicle in short computational time. Successful scalability testing of the integrated and parallelized software system was carried out on the TARDEC HPC [39] to learn how to achieve the computational speed-up.

With the success of the MPP-based RBDO methods and software tools, the Iowa team started extending them by developing a sampling-based system level RBDO method [40,41] to support broader ground vehicle applications as shown in Fig. 3. For the sampling-based RBDO, the stochastic sensitivity analysis [40] is developed to compute sensitivities of probabilistic constraints with respect to independent and correlated random design variables; and the Dynamic Kriging (DKG) method is developed for surrogate modeling [42].

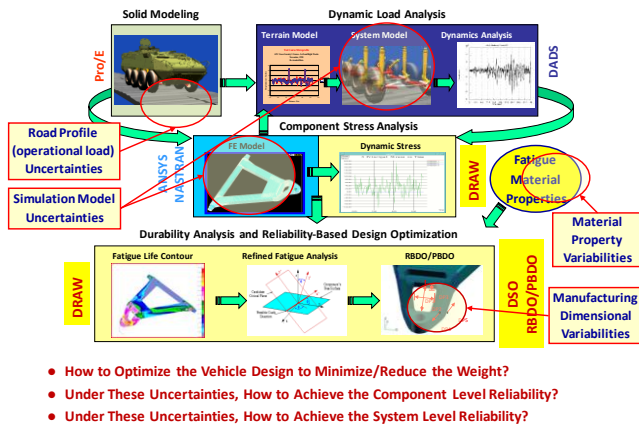


Figure 1. Ground Vehicle RBDO Process for Durability, Reliability, and Weight Reduction

Over the years, the University of Iowa and U.S. Army Tank Automotive Research, Development, and Engineering Center (TARDEC) have been working together to develop a simulation-based RBDO process to minimize the Army ground vehicle weight while maintaining/improving durability and system-level reliability requirements, as shown in Fig. 1. The durability analysis process that predicts fatigue failure of the ground vehicle components due to cyclic damage accumulations is a multidisciplinary simulation process, requiring an integration of a CAD tool and several CAE tools, such as multibody dynamic analysis, FEA, and durability analysis; and a large amount of data communication as shown in Fig. 1. In addition, the design sensitivity analysis (DSA) [24,25] of the fatigue life with respect to the design variables (random or deterministic) and

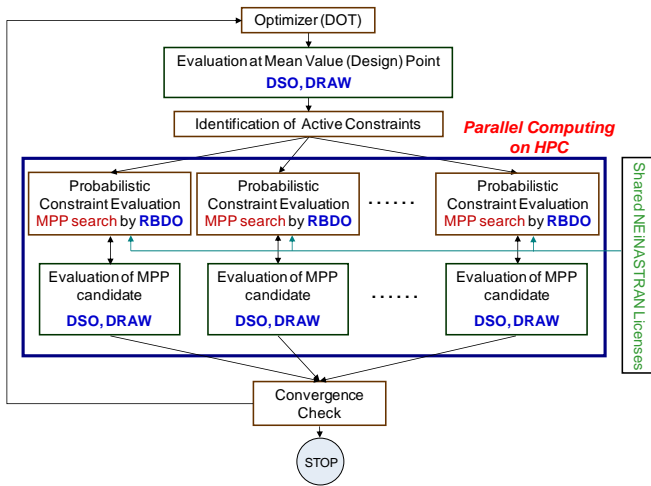


Figure 2. Parallelized DRAW-DSO-RBDO Integrated Software System on TARDEC HPC

For Broader Applications of Modeling & Simulation-Based RBDO, Each Discipline Needs to Develop Sensitivity Method

- Vehicle Weight Reduction and Durability
- Advanced & Hybrid Powertrain
- Electric Power & On-Board Electrification
- Robotic Systems
- Safety Analysis for Survivability & Design
- Human Centered Design
- Noise & Vibration
- Crashworthiness
- Manufacturing Processes
- MEMS & Microelectronics Packaging
- Nano & Micromechanics Based Materials Modeling, ..., Etc.

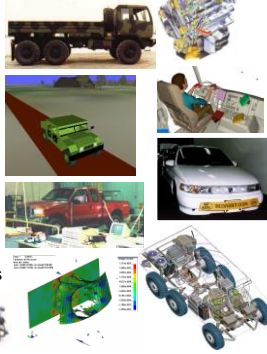


Figure 3. Future Goals: Broader Applications of Reliability-Based Design Optimization

2. DYNAMIC KRIGING METHOD

In the Kriging method, the outcomes are considered as a realization of a stochastic process, and the predicted values are derived by applying the stochastic process theory. Consider n sample points with $\mathbf{X} = [\mathbf{x}_1, \mathbf{x}_2, \dots, \mathbf{x}_n]^T$, $\mathbf{x}_i \in \mathbf{R}^m$, and n responses $\mathbf{y} = [y(\mathbf{x}_1), y(\mathbf{x}_2), \dots, y(\mathbf{x}_n)]^T$ with $y(\mathbf{x}_i) \in \mathbf{R}^1$. Thus, the responses at samples are considered as a summation of two parts as

$$\mathbf{y} = \mathbf{F}\boldsymbol{\beta} + \mathbf{e} \quad (1)$$

In Eq. (1), $\mathbf{F}\boldsymbol{\beta}$ is the mean structure of the response, where $\mathbf{F} = [f_k(\mathbf{x}_i)]$, $i = 1, \dots, n$, $k = 1, \dots, K$, is an $n \times K$ design matrix;

and $f_k(\mathbf{x})$, $k = 1, \dots, K$, represent the basis functions, which are usually in a simple polynomial form, such as $1, x, x^2, \dots$. Also, $\boldsymbol{\beta} = [\beta_1, \beta_2, \dots, \beta_K]^T$ is the vector of regression coefficients; and $\mathbf{e} = [e(\mathbf{x}_1), e(\mathbf{x}_2), \dots, e(\mathbf{x}_n)]^T$ is a realization of the stochastic process $e(\mathbf{x})$ that is assumed to have zero mean $E[e(\mathbf{x}_i)] = 0$. The covariance structure is $E[e(\mathbf{x}_i)e(\mathbf{x}_j)] = \sigma^2 R(\boldsymbol{\theta}, \mathbf{x}_i, \mathbf{x}_j)$, where σ^2 is the process variance; $\boldsymbol{\theta} = (\theta_1, \theta_2, \dots, \theta_{nr})$ is the correlation parameter vector that has to be estimated by applying the maximum likelihood estimator (MLE); and $R(\boldsymbol{\theta}, \mathbf{x}_i, \mathbf{x}_j)$ is the correlation function of the stochastic process [43]. Usually, the correlation function is set to Gaussian form in engineering applications and expressed as

$$R(\boldsymbol{\theta}, \mathbf{x}_i, \mathbf{x}_j) = \prod_{l=1}^{nr} \exp(-\theta_l (x_{i,l} - x_{j,l})^2) \quad (2)$$

where $x_{i,l}$ is the l^{th} component of variable \mathbf{x}_i . Under the decomposition of Eq. (1) and $\boldsymbol{\theta}$, which is obtained to maximize MLE,

$$L = (2\pi\sigma^2)^{-\frac{n}{2}} |\mathbf{R}|^{-\frac{1}{2}} \exp\left[-\frac{1}{2\sigma^2} (\mathbf{y} - \mathbf{F}\boldsymbol{\beta})^T \mathbf{R}^{-1} (\mathbf{y} - \mathbf{F}\boldsymbol{\beta})\right] \quad (3)$$

where \mathbf{R} is the symmetric correlation matrix with i - j^{th} component $R_{ij} = R(\boldsymbol{\theta}, \mathbf{x}_i, \mathbf{x}_j)$, $i, j = 1, \dots, n$, and

$\sigma^2 = \frac{1}{n} (\mathbf{y} - \mathbf{F}\boldsymbol{\beta})^T \mathbf{R}^{-1} (\mathbf{y} - \mathbf{F}\boldsymbol{\beta})$ and $\boldsymbol{\beta} = (\mathbf{F}^T \mathbf{R}^{-1} \mathbf{F})^{-1} \mathbf{F}^T \mathbf{R}^{-1} \mathbf{y}$ are obtained from the generalized least square regression.

The objective of the Kriging method is to predict the noise-free unbiased response at a new point of interest denoted by \mathbf{x} . This prediction of response at \mathbf{x} is written as a linear predictor as

$$y_{krig}(\mathbf{x}) = \mathbf{w}^T \mathbf{y} \quad (4)$$

where $\mathbf{w} = [w_1(\mathbf{x}), w_2(\mathbf{x}), \dots, w_n(\mathbf{x})]^T$ denotes the $n \times 1$ weight vector for prediction at \mathbf{x} and is obtained using the unbiased condition $E[y_{krig}(\mathbf{x})] = E[y(\mathbf{x})]$ as [42]

$$\mathbf{w} = \mathbf{R}^{-1} (\mathbf{r} + \frac{1}{2\sigma^2} \mathbf{F}\boldsymbol{\lambda}) \quad (5)$$

where $\boldsymbol{\lambda}$ is the Lagrange multiplier; and $\mathbf{r} = [R(\boldsymbol{\theta}, \mathbf{x}_1, \mathbf{x}), \dots, R(\boldsymbol{\theta}, \mathbf{x}_n, \mathbf{x})]^T$ is the correlation vector between \mathbf{x} and samples \mathbf{x}_i , $i = 1, \dots, n$.

Under the assumption of the Gaussian process, the $1-\alpha$ level prediction interval of the response is obtained as

$$y_{krig}(\mathbf{x}) - Z_{1-\alpha/2} \sigma_p(\mathbf{x}) \leq y(\mathbf{x}) \leq y_{krig}(\mathbf{x}) + Z_{1-\alpha/2} \sigma_p(\mathbf{x}) \quad (6)$$

where $Z_{1-\alpha/2}$ is the $1-\alpha$ level quantile of the standard normal distribution and $\sigma_p^2(\mathbf{x})$ is the predicted variance at \mathbf{x} given by $\sigma_p^2(\mathbf{x}) = \sigma^2(1 + \mathbf{u}^T(\mathbf{F}^T\mathbf{R}^{-1}\mathbf{F})^{-1}\mathbf{u} - \mathbf{r}^T\mathbf{R}^{-1}\mathbf{r})$. Therefore, the bandwidth of the prediction interval at a point of interest \mathbf{x}_0 is

$$d(\mathbf{x}) = 2Z_{1-\alpha/2}\sigma_p(\mathbf{x}) \quad (7)$$

and this prediction interval will be used as an accuracy measure to decide if the surrogate model is accurate or not.

Depending on the basis functions $f_k(\mathbf{x})$ used in Eq. (1), the Kriging method is called the ordinary Kriging method, first-order universal Kriging method, and second-order universal Kriging method, where basis functions with constant terms only, up to first-order polynomial terms, and up to second-order polynomial terms, respectively, are used. For both the ordinary and universal Kriging methods, the basis functions do not change during the surrogate model generation process. However, in general, the higher-order terms can predict the nonlinear mean structure, and thus fixed-order basis functions may not be good to describe the nonlinearity of the mean structure. On the other hand, it is also known that, in some cases, the accuracy of the surrogate model may deteriorate by using higher-order terms [44]. Therefore, it is desirable to find the optimal set of polynomial basis functions that could provide the most accurate surrogate model.

First, the Dynamic Kriging (DKG) method dynamically selects the optimal set of basis functions at each design point so that the generated surrogate model has the best accuracy. As explained above, the accuracy is measured using the prediction interval bandwidth in Eq. (7). To apply the DKG method to find the best basis function set, the highest-order P must first be determined. With n samples given, Eq. (4) can be solved when the total number of basis functions is less than n , that is,

$$\binom{P}{nd+P} \leq n-1. \quad (8)$$

The highest order P of the polynomial that satisfies Eq. (8) is determined. For example, if 10 samples are given ($n=10$) for a 2-D problem, the highest-order P will be 3 to satisfy Eq. (8) so that we can have basis functions up to third-order polynomials as 1, x_1 , x_2 , x_1x_2 , x_1^2 , x_2^2 , $x_1^2x_2$, $x_1x_2^2$, x_1^3 , and x_2^3 . After deciding the highest-order P , the genetic algorithm (GA) is used to find the best basis function set by minimizing the Kriging process variance

$$\sigma^2 = \frac{1}{n}(\mathbf{y} - \mathbf{F}\boldsymbol{\beta})^T \mathbf{R}^{-1}(\mathbf{y} - \mathbf{F}\boldsymbol{\beta}).$$

Second, a generalized pattern search algorithm is used to find the optimal correlation parameter $\boldsymbol{\theta}$ to maximize the MLE in Eq. (3). Since it is not a gradient-based optimization method and guarantees the global convergence,

which is proven by Lewis and Torczon [45], the pattern search algorithm is powerful enough to find the optimal $\boldsymbol{\theta}$.

Using the GA for the best basis function set and the pattern search for the optimal $\boldsymbol{\theta}$, the studied examples show that the DKG method outperforms existing surrogate model generation methods including the universal Kriging method, the polynomial response surface method, the radial basis function method, the support vector regression method, and the blind Kriging method [42].

3. SAMPLING-BASED RBDO

The mathematical formulation of a general RBDO problem is expressed as

$$\begin{aligned} & \text{minimize} && \text{Cost}(\mathbf{d}) \\ & \text{subject to} && P[G_j(\mathbf{X}) > 0] \leq P_{F_j}^{\text{Tar}}, \quad j=1, \dots, nc \\ & && \mathbf{d}^L \leq \mathbf{d} \leq \mathbf{d}^U, \quad \mathbf{d} \in \mathbf{R}^{nd} \text{ and } \mathbf{X} \in \mathbf{R}^{nr} \end{aligned} \quad (9)$$

where $\mathbf{d} = \{d_i\}^T = \boldsymbol{\mu}(\mathbf{X}^{\text{rv}})$, $i=1 \sim nd$ is the design vector, which is the mean value of the nd -dimensional random variable vector $\mathbf{X}^{\text{rv}} = \{X_1, X_2, \dots, X_{nd}\}^T$; $\mathbf{X} = \{\mathbf{X}^{\text{rv}}, \mathbf{X}^{\text{rp}}\}^T$ where \mathbf{X}^{rv} and \mathbf{X}^{rp} stand for the random design variable and random parameter components of the random input \mathbf{X} , respectively; $P_{F_j}^{\text{Tar}}$ is the target probability of failure for the j^{th} constraint; and nc , nd , and nr are the number of probabilistic constraints, design variables, and random variables plus parameters, respectively.

A reliability analysis for both the component and system levels involves calculation of the probability of failure, denoted by P_F , which is defined using a multi-dimensional integral as

$$\begin{aligned} P_F(\boldsymbol{\psi}) &\equiv P[\mathbf{X} \in \Omega_F] = \int_{\mathbf{R}^{nr}} I_{\Omega_F}(\mathbf{x}) f_{\mathbf{X}}(\mathbf{x}; \boldsymbol{\psi}) d\mathbf{x} \\ &= E[I_{\Omega_F}(\mathbf{X})] \end{aligned} \quad (10)$$

where $\boldsymbol{\psi}$ is a vector of distribution parameters, which usually includes the mean ($\boldsymbol{\mu}$) and/or standard deviation ($\boldsymbol{\sigma}$) of the random input $\mathbf{X} = \{X_1, \dots, X_{nr}\}^T$; $P[\bullet]$ represents a probability measure; Ω_F is the failure set; $f_{\mathbf{X}}(\mathbf{x}; \boldsymbol{\psi})$ is a joint probability density function (PDF) of \mathbf{X} ; and $E[\bullet]$ represents the expectation operator. The failure set is defined as $\Omega_{F_j} \equiv \{\mathbf{x} : G_j(\mathbf{x}) > 0\}$ for component reliability analysis of the j^{th} constraint function $G_j(\mathbf{x})$, and $\Omega_F \equiv \{\mathbf{x} : \bigcup_{j=1}^{nc} G_j(\mathbf{x}) > 0\}$ and $\Omega_F \equiv \{\mathbf{x} : \bigcap_{j=1}^{nc} G_j(\mathbf{x}) > 0\}$ for the series system and parallel system reliability analysis of nc performance functions, respectively. $I_{\Omega_F}(\mathbf{x})$ in Eq. (10) is called an indicator function and defined as

$$I_{\Omega_F}(\mathbf{x}) \equiv \begin{cases} 1, & \mathbf{x} \in \Omega_F \\ 0, & \text{otherwise} \end{cases} \quad (11)$$

In this paper, since the mean of \mathbf{X} , $\boldsymbol{\mu} = \{\mu_1, \dots, \mu_{nd}\}^T$ is used as a design vector, the vector of distribution parameters $\boldsymbol{\psi}$ is simply replaced with $\boldsymbol{\mu}$ for the computation of the probability of failure in Eq. (10).

Taking the partial derivative of probability of failure in Eq. (10) with respect to the i^{th} design variable μ_i yields

$$\frac{\partial P_F(\boldsymbol{\mu})}{\partial \mu_i} = \frac{\partial}{\partial \mu_i} \int_{\mathbf{R}^{nr}} I_{\Omega_F}(\mathbf{x}) f_{\mathbf{X}}(\mathbf{x}; \boldsymbol{\mu}) d\mathbf{x} \quad (12)$$

and the differential and integral operators can be interchanged using the Leibniz's rule, giving

$$\begin{aligned} \frac{\partial P_F(\boldsymbol{\mu})}{\partial \mu_i} &= \int_{\mathbf{R}^{nr}} I_{\Omega_F}(\mathbf{x}) \frac{\partial f_{\mathbf{X}}(\mathbf{x}; \boldsymbol{\mu})}{\partial \mu_i} d\mathbf{x} \\ &= \int_{\mathbf{R}^{nr}} I_{\Omega_F}(\mathbf{x}) \frac{\partial \ln f_{\mathbf{X}}(\mathbf{x}; \boldsymbol{\mu})}{\partial \mu_i} f_{\mathbf{X}}(\mathbf{x}; \boldsymbol{\mu}) d\mathbf{x} \\ &= E \left[I_{\Omega_F}(\mathbf{x}) \frac{\partial \ln f_{\mathbf{X}}(\mathbf{x}; \boldsymbol{\mu})}{\partial \mu_i} \right] \end{aligned} \quad (13)$$

since $I_{\Omega_F}(\mathbf{x})$ is not a function of μ_i . The partial derivative of the log function of the joint PDF in Eq. (13) with respect to μ_i is known as the first-order score function for μ_i and is denoted as

$$s_{\mu_i}^{(1)}(\mathbf{x}; \boldsymbol{\mu}) \equiv \frac{\partial \ln f_{\mathbf{X}}(\mathbf{x}; \boldsymbol{\mu})}{\partial \mu_i}. \quad (14)$$

To compute the probability of failure in Eq. (10) and the sensitivity of probability of failure in Eq. (13), statistical sampling such as the Monte Carlo simulation (MCS) at a given design needs to be applied to true responses, which is computationally very expensive and almost prohibited. Hence, instead of using the true responses, which are usually obtained from computer simulations, the surrogate models obtained using the DKG method are used.

Denote the surrogate model obtained by the DKG method for the constraint function $G_j(\mathbf{X})$ as $\hat{G}_j(\mathbf{X})$. Then, by carrying out the MCS using the conservative surrogate model $\hat{G}_j(\mathbf{X})$, the probabilistic constraints in Eq. (9) can be approximated as

$$P_{F_j} \equiv P[G_j(\mathbf{X}) > 0] \cong \frac{1}{M} \sum_{m=1}^M I_{\hat{\Omega}_{F_j}}(\mathbf{x}^{(m)}) \leq P_{F_j}^{\text{Tar}} \quad (15)$$

where M is the MCS sample size, $\mathbf{x}^{(m)}$ is the m^{th} realization of \mathbf{X} , and the failure set $\hat{\Omega}_{F_j}$ for the surrogate model is defined as $\hat{\Omega}_{F_j} \equiv \{\mathbf{x} : \hat{G}_j(\mathbf{x}) > 0\}$. Sensitivity of the probabilistic constraint in Eq. (13) is obtained as

$$\frac{\partial P_{F_j}}{\partial \mu_i} \cong \frac{1}{M} \sum_{m=1}^M I_{\hat{\Omega}_{F_j}}(\mathbf{x}^{(m)}) s_{\mu_i}^{(1)}(\mathbf{x}^{(m)}; \boldsymbol{\mu}) \quad (16)$$

where $s_{\mu_i}^{(1)}(\mathbf{x}^{(m)}; \boldsymbol{\mu})$ is obtained using Eq. (14).

4. PARALLELIZATION OF SAMPLING-BASED RBDO

As explained in Section 2, the DKG method uses the pattern search and genetic algorithm for more accurate surrogate model generation. Hence, as the dimension of the complex engineering system increases, the DKG method and MCS for the reliability analysis using surrogate models become computationally inefficient. Moreover, the number of samples required for computer simulations increases. Therefore, a high performance computing strategy needs to be implemented into the sampling-based RBDO procedure to ensure it is applicable for large-scale complex engineering applications.

For the sampling-based RBDO using the DKG method, there exist three major places where the parallel computing can be applicable: parallelization of surrogate model generation for multiple constraints, parallelization of MCS for multiple surrogate models, and parallelization of computer simulations at samples. The Matlab parallel computing toolbox and the parallel computing platform (LSF-Platform) are utilized for the first two parallelizations and for the last parallelization, respectively, of the sampling-based RBDO with the DKG method.

Compared with the gradient-based or MPP-based RBDO, the sampling-based RBDO has inherent advantages in terms of the parallelization. In the MPP-based RBDO, the parallelization is limited to the number of constraints (nc), which means that even if numerous client computers are available it can only use nc client computers for the parallelized computing. On the other hand, the sampling-based RBDO can use as many client computers as the number of samples, which is usually more than the number of constraints for high dimensional problems. In addition, the sampling-based RBDO has more places where the parallelization can be applicable. Hence, in terms of the parallel computing, the sampling-based RBDO is more effective than the MPP-based RBDO [39].

4.1 Parallelization of Surrogate Models for Multiple Constraints in RBDO

A typical RBDO problem contains more than one constraint. Since the surrogate model from the DKG method is computationally expensive for high dimensional large-scale applications, it is desirable to carry out the surrogate modeling for all constraints simultaneously, which leads to the parallelization of surrogate modeling for multiple constraints. This parallelization is conducted by using the Matlab parallel computing tool-box.

4.2 Parallelization of MCS in Reliability Analysis

The MCS in the sampling-based RBDO is used to calculate failure probabilities of performance functions as well as their sensitivities with respect to design variables. Usually, MCS requires a large number of samples for accurate results. Moreover, since the prediction from the DKG method at the MCS samples is implicit, a large dimension matrix calculation is involved every time the prediction is calculated at each MCS point. As the number of the MCS samples increases, the total computational time for the reliability and sensitivity analysis increases as well. Therefore, the parallelization of the MCS procedure is also needed to reduce the large computational time. This parallelization is also conducted by using the Matlab parallel computing toolbox.

4.3 Parallelization of Computer Aided Engineering (CAE) at Samples

To generate surrogate models of the performance functions in RBDO by the DKG method, it is required to evaluate the performance functions at the sample points, which is usually conducted by computer simulation. This procedure is computationally intensive for large-scale complex engineering applications. If the number of the computer simulations is large for a large-scale engineering application, apparently, the total computational time of conducting the computer simulations for all samples may become unaffordable. Therefore, the parallelization is necessary for this procedure. Usually the computer simulation is carried out by general CAE commercial software and the parallelization can be done by the parallel computing platform (LSF-Platform).

4.4 Summary of Parallelization in Sampling-Based RBDO

With all the discussion above, we can obtain the entire workflow of the parallelization in the sampling-based RBDO shown in Fig. 4, where a “core” means a unit in a multiple-core desktop and a “node” means one client computer in a cluster network.

5. NUMERICAL EXAMPLES

This section illustrates two design optimization examples – a 2-D mathematical example and a 12-D M1A1 Abrams tank roadarm – to see how the proposed sampling-based RBDO works for an RBDO problem. The 2-D mathematical example is used to show the accuracy and efficiency of the proposed method since its analytic functions are available, and thus the MCS is applicable for the comparison of the probability of failure calculation. The 12-D M1A1 Abrams tank roadarm is used to see how the proposed sampling-based RBDO works for a high-dimensional engineering application in terms of accuracy and efficiency. In addition,

using the roadarm example, the effectiveness of the parallelization is also explained. For all examples, 1 million testing points are used for the DKG method, and 500,000 MCS samples are used for the reliability and sensitivity analysis and the MCS sample number increases to 1 million when constraints are identified as active.

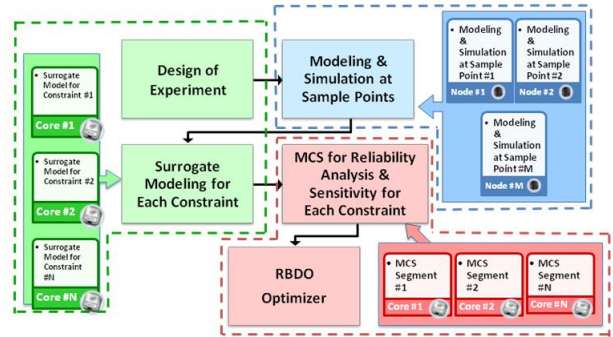


Figure 4. Workflow of Parallelization in RBDO

5.1 RBDO of 2-D Mathematical Problem

Consider a 2-D mathematical RBDO problem, which is formulated to

$$\begin{aligned} \text{minimize} \quad & \text{Cost}(\mathbf{d}) = -\frac{(d_1 + d_2 - 10)^2}{30} - \frac{(d_1 - d_2 + 10)^2}{120} \\ \text{subject to} \quad & P(G_j(\mathbf{X}(\mathbf{d})) > 0) \leq P_F^{\text{Tar}} = 2.275\%, \quad j = 1 \sim 3 \quad (17) \\ & \mathbf{d}^l \leq \mathbf{d} \leq \mathbf{d}^u, \quad \mathbf{d} \in \mathbf{R}^2 \text{ and } \mathbf{X} \in \mathbf{R}^2 \end{aligned}$$

where three constraint functions are expressed as

$$\begin{aligned} G_1(\mathbf{X}) &= 1 - \frac{X_1^2 X_2}{20} \\ G_2(\mathbf{X}) &= -1 + (Y - 6)^2 + (Y - 6)^3 - 0.6 \times (Y - 6)^4 + Z \quad (1) \\ G_3(\mathbf{X}) &= 1 - \frac{80}{X_1^2 + 8X_2 + 5} \end{aligned}$$

where $\begin{Bmatrix} Y \\ Z \end{Bmatrix} = \begin{bmatrix} 0.9063 & 0.4226 \\ 0.4226 & -0.9063 \end{bmatrix} \begin{Bmatrix} X_1 \\ X_2 \end{Bmatrix}$, and are drawn in Fig.

5. The properties of two random variables are shown in Table 5, and they are correlated with the Clayton copula ($\tau=0.5$). As shown in Eq. (17), the target probability of failure (P_F^{Tar}) is 2.275% for all constraints.

As shown in Fig. 5 and Table 1, the initial design is $\mathbf{d}^0 = [5, 5]^T$. At the initial design, the sampling-based deterministic design optimization (DDO) is first used to find the deterministic optimum, which is usually close to the RBDO optimum, and the sampling-based RBDO is launched at the deterministic optimum design. This approach is more computationally efficient than launching the RBDO from the beginning. As shown in Fig. 6, the DDO requires 30

samples, which are marked as asterisks in the figure, for the whole design iteration, and the deterministic optimum design is exactly identical to the optimum design obtained using analytic functions in Eq. (17). At the deterministic optimum, the sampling-based RBDO is launched, with a total of 18 samples are initially used for the first iteration of the sampling-based RBDO. Twenty more samples, which are marked as dots in Fig. 6, are generated for the sampling-based RBDO whose result is shown in Table 2.

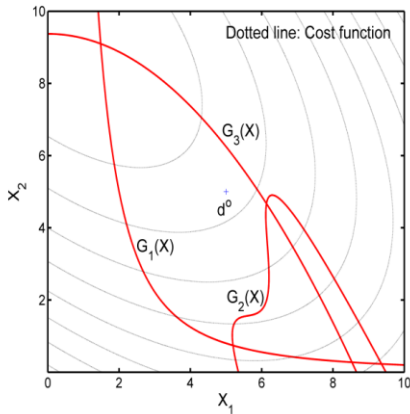


Figure 5. Shape of Constraint Functions

Table 1. Properties of Random Variables

Random Variables	Distribution	d^L	d^0	d^U	Standard Deviation
X_1	Normal	0.0	5.0	10.0	0.3
X_2	Normal	0.0	5.0	10.0	0.3

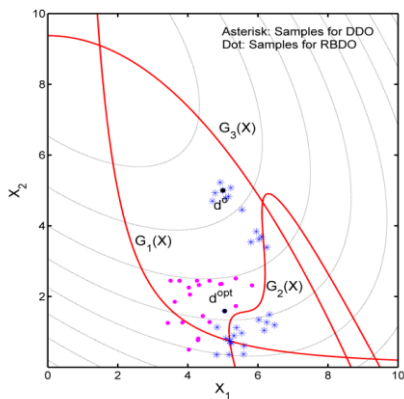


Figure 6. Sample Profile for DDO and RBDO

Table 2 compares the numerical results of five different RBDO methods. The first three results are obtained from the MPP-based RBDO, which requires sensitivities of constraint functions for the MPP search and design

optimization. This MPP-based RBDO includes the FORM [14] and the DRM [19] with three and five quadrature points, which are denoted in Table 2 as DRM3 and DRM5, respectively. The results of the last two rows are obtained from the sampling-based RBDO, which uses the MCS for the estimation of the probability of failure and its sensitivity. The sampling-based RBDO using the DKG method is the proposed method, and to compare the accuracy of the proposed method, the result of the sampling-based RBDO using the analytic (true) functions given in Eq. (35) is also shown in the table.

From the table, it can be seen that the probability of failure of the second constraint (1.2835%) estimated by the MCS with 50 million samples at the optimum design obtained using the FORM is not close to the target probability of failure (2.275%). This is because the second constraint is highly nonlinear as shown in Fig. 6, and the FORM uses the transformation from original X-space to standard normalized U-space, which makes the constraint even more highly nonlinear due to the correlated nonlinear input. For highly nonlinear functions, the FORM cannot accurately estimate the probability of failure since it uses the linear approximation of the nonlinear functions at the MPP in U-space. To improve the accuracy of the probability of failure at the optimum design, the MPP-based DRM with three or five quadrature points can be used [19]; Table 2 shows that the MPP-based DRM indeed improves the accuracy of the probability of failure at the optimum design with more function evaluations. However, to obtain a more accurate optimum design, more quadrature points are required, such as the DRM7, etc. To obtain the optimum design, the FORM uses 52 function evaluations and $52 \times 2 = 104$ sensitivity calculations, whereas the MPP-based DRM with five quadrature points uses 146 function evaluations and $102 \times 2 = 104$ sensitivity calculations, and the number of function evaluations for the MPP-based DRM will be increased as the number of quadrature points increases [19].

Table 2. Comparison of Various RBDOs ($P_F^{tar} = 2.275\%$)

Methods	Cost	Optimum Design	MCS (50M)		Number of Function Evaluations
			$P_{F1}, \%$	$P_{F2}, \%$	
MPP-Based RBDO	FORM	-1.8742, 5.0026, 1.6165	2.3022	1.2835	$52 + 52 \times 2$
	DRM3	-1.8794, 5.0315, 1.6050	2.2912	1.7496	$128 + 106 \times 2$
	DRM5	-1.8821, 5.0454, 1.5988	2.2621	2.0183	$146 + 102 \times 2$
Sampling-Based RBDO	DKG	-1.8845, 5.0576, 1.5936	2.2716	2.2869	50
	Analytic Function	-1.8853, 5.0541, 1.5918	2.2912	2.2791	N.A.

On the other hand, the sampling-based RBDO shows very accurate optimum design since the optimum design is very

close to the optimum design obtained using the analytic functions. However, it requires only 50 samples, which is even less than the FORM, for the accurate optimum design without requiring the sensitivity of the performance functions. The sampling-based RBDO can obtain a very accurate optimum design because it does not use any approximation on the calculation of the probability of failure, unlike the FORM and MPP-based DRM, and the DKG method generates very accurate surrogate models. In addition, it can be said that the proposed efficiency strategies indeed work in this example. Therefore, once surrogate models for constraint functions are accurate enough, the proposed sampling-based RBDO could obtain a very accurate optimum design with good efficiency.

5.2 RBDO of M1A1 Abrams Tank Roadarm

The roadarm of the M1A1 Abrams tank [19] is used to compare two approaches: the MPP-based RBDO, which requires sensitivities of performance functions, and the sampling-based RBDO, which does not require sensitivities of performance functions, for the component RBDO. The roadarm is modeled using 1572 eight-node isoparametric finite elements (SOLID45) and four beam elements (BEAM44) of ANSYS [46], as shown in Fig. 7, and is made of S4340 steel with Young’s modulus $E=3.0 \times 10^7$ psi and Poisson’s ratio $\nu=0.3$. The durability analysis of the roadarm is carried out using Durability and Reliability Analysis Workspace (DRAW) [26] to obtain the fatigue life contour. The fatigue lives at the critical nodes are shown in Fig. 8, which are chosen as the design constraints of the RBDO.

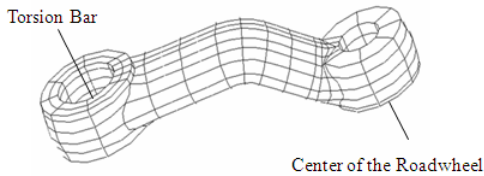


Figure 7. Finite Element Model of Roadarm

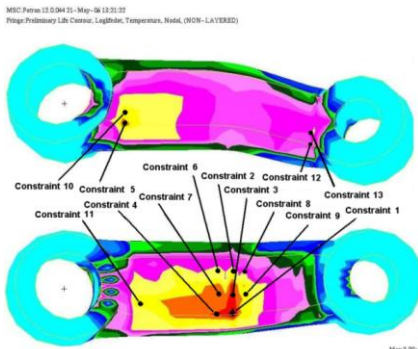


Figure 8. Fatigue Life Contour at Critical Nodes of Roadarm

The shape design variables are shown in Fig. 9. Eight shape design variables characterize four cross-sectional shapes of the roadarm. The widths (x_1 -direction) of the cross-sectional shapes are defined by the design variables $d_1, d_3, d_5,$ and d_7 at intersections 1, 2, 3, and 4, respectively, and the heights (x_3 -direction) of the cross-sectional shapes are defined using the remaining four design variables. Eight shape design variables are listed in Table 3 and are assumed to be independent random variables.

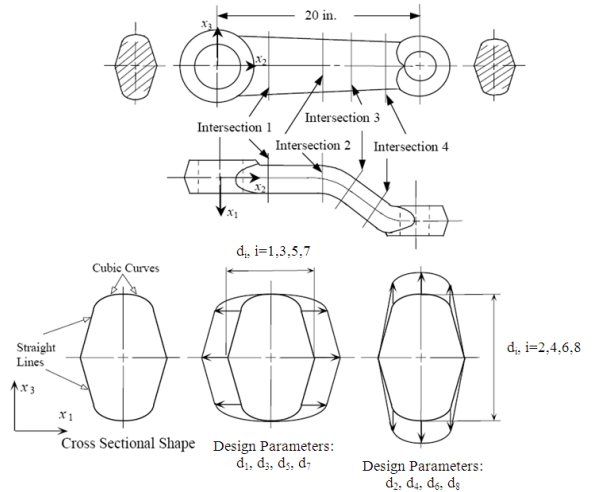


Figure 9. Shape Design Variables for Roadarm

For the input fatigue material properties, since the statistical information on S4340 steel other than its nominal value is not available, it is necessary to assume the statistical information on S4340 steel. The strain-life relationship is given by the classical Coffin-Manson equation as [47]

$$\frac{\Delta \epsilon}{2} = \frac{\Delta \epsilon_e}{2} + \frac{\Delta \epsilon_p}{2} = \frac{\sigma'_f}{E} (2N_f)^{b_s} + \epsilon'_f (2N_f)^{c_d} \quad (19)$$

where σ'_f and b_s are the fatigue strength coefficient and exponent, respectively; ϵ'_f and c_d are the fatigue ductility coefficient and exponent, respectively; N_f is the fatigue initiation life; and E is the Young’s modulus. It is known that σ'_f and ϵ'_f follow the lognormal distribution and b_s and c_d follow the normal distribution. Furthermore, it is also known that $\sigma'_f, b_s,$ and ϵ'_f, c_d are highly negatively correlated [22]. For the correlated fatigue material properties, it is assumed that σ'_f and b_s follow the Gaussian copula with $\rho=-0.828$ and that ϵ'_f and c_d follow the Frank copula with $\tau=-0.906$ [22]. For the standard deviations of

S4340 steel, 3% coefficients of variation (COV) for fatigue material properties are assumed as shown in Table 3. It is known that fatigue strength parameters and fatigue ductility parameters are not correlated each other.

Table 3. Random Variables and Fatigue Material Properties

Random Variables	Lower Bound \mathbf{d}^L	Initial Design \mathbf{d}^0	Upper Bound \mathbf{d}^U	COV	Distribution Type
d_1 , in.	1.350	1.750	2.150	1%	Normal
d_2 , in.	2.650	3.250	3.750		
d_3 , in.	1.350	1.750	2.150		
d_4 , in.	2.570	3.170	3.670		
d_5 , in.	1.356	1.756	2.156		
d_6 , in.	2.438	3.038	3.538		
d_7 , in.	1.352	1.752	2.152		
d_8 , in.	2.508	2.908	3.408		
Fatigue Material Properties					
Non-design Uncertainties			Mean	COV	Distribution Type
Fatigue Strength Coefficient, σ_f' , psi			177000		Lognormal
Fatigue Strength Exponent, b_s			-0.0730	3%	Normal
Fatigue Ductility Coefficient, ϵ_f'			0.4100		Lognormal
Fatigue Ductility Exponent, c_d			-0.6000		Normal

The RBDO for the M1A1 Abrams tank roadarm is formulated to

$$\begin{aligned} & \text{minimize} \quad \text{Cost}(\mathbf{d}) \\ & \text{subject to} \quad P[G_j(\mathbf{X}) > 0] \leq P_F^{\text{Tar}}, \quad j = 1, \dots, 13 \quad (20) \\ & \quad \mathbf{d}^L \leq \mathbf{d} \leq \mathbf{d}^U, \quad \mathbf{d} \in \mathbf{R}^8 \text{ and } \mathbf{X} \in \mathbf{R}^{12} \end{aligned}$$

where

$$\begin{aligned} & \text{Cost}(\mathbf{d}) : \text{Weight of Roadarm} \\ & G_j(\mathbf{d}) = 1 - \frac{L(\mathbf{d})}{L_i}, \quad j = 1 \sim 13 \\ & L(\mathbf{d}) : \text{Crack Initiation Fatigue Life}, \quad (21) \\ & L_i : \text{Crack Initiation Target Fatigue Life (=5 years)} \\ & P_F^{\text{Tar}} = 2.275\% \end{aligned}$$

For the sampling-based DDO, 15 samples are used as the initial number of samples in the local window. Smaller local window is used for the DDO since the accuracy of the surrogate model near a given design is required for sensitivity calculation and there is no need of reliability analysis. After 11 iterations, the sampling-based DDO converged to the optimum design, using 135 samples. The optimum design obtained using the sampling-based DDO is almost identical with the optimum design obtained using the sensitivity-based DDO as shown in Table 4. The sensitivity-based DDO requires 11 function and 11 sensitivity evaluations as shown in Table 4, where F.E. stands for ‘function evaluation’. One sensitivity evaluation includes

sensitivity calculations for all design variables, so it requires $11 \times 8 = 88$ sensitivity calculations in this example, whereas the sampling-based DDO requires a total of 135 samples for the surrogate model generation using the DKG method.

Table 4. Comparison of Optimum Designs

Design Variable	Initial	Sensitivity-Based		Sampling-Based	
		DDO	RBDO	DDO	RBDO
d_1	1.750	1.653	1.711	1.653	1.705
d_2	3.250	2.650	2.650	2.650	2.650
d_3	1.750	1.922	1.943	1.922	1.941
d_4	3.170	2.570	2.570	2.570	2.570
d_5	1.756	1.478	1.514	1.478	1.508
d_6	3.038	3.287	3.348	3.287	3.352
d_7	1.752	1.630	1.691	1.630	1.702
d_8	2.908	2.508	2.508	2.508	2.508
# of F.E.		11+11×8	85+85×12	135	691
Active Constraints		1,3,5,8,12	1,3,5,8,12	1,3,5,8,12	1,3,5,8,12
Cost	515.09	466.80	474.20	466.81	474.60

The sampling-based RBDO is launched at the DDO. In this case, samples used for the DDO cannot be used for the RBDO unlike the mathematical example because the dimension of the DDO is 8, whereas the dimension of the RBDO is 12. The number of initial samples within the local window is 200. It is found that 4 out of 13 performance functions are very feasible at the deterministic optimum. Hence, surrogate models for those performance functions are not generated to save the computation time. Table 4 also compares two RBDO optimum designs obtained using the sensitivity-based and sampling-based RBDO. The FORM is used for the sensitivity-based RBDO.

From the table, it can be seen that two optimum designs are very close to each other. At the optimum design obtained using the sampling-based RBDO, the MSE of the surrogate model is 0.0062, which is much less than the target MSE (0.01) and means that surrogate model at the optimum design is accurate enough. To obtain the optimum design using the FORM, 85 function and $85 \times 12 = 1020$ sensitivity evaluations are used since there exist 8 random design variables and 4 random parameters, whereas the sampling-based RBDO uses 691 samples, which means 691 function evaluations, to find the optimum design.

5.3 Efficiency of Parallel Computing

It is noted that one license of the Matlab parallel computing toolbox allows 8 cores working simultaneously, therefore 8 surrogate models for constraints are generated at the same time. Thus, using the parallelization explained in Sections 4.1 and 4.2, the computation time is maximally 8 times faster than the one without the parallelization. However, the number of cores used for the parallelization

can be extended if parallel computing software other than the Matlab toolbox is utilized.

To demonstrate the improvement of the efficiency by applying the parallelization to the sampling-based RBDO using the DKG method, the same M1A1 Abrams tank roadarm example in Section 5.2 is used. The comparison between the parallel computing and the original serial computing is carried out by running the reliability analysis at the deterministic optimum design with 250 points in the local window. Nine constraints are identified as active or violated constraints at the deterministic optimum design and thus surrogate models are generated for those 9 constraints only.

As shown in Table 5, the parallel computing reduces the computational time by 72.7% for surrogate modeling and 67.4% for the MCS. The reason that the reduction of the computational time for the surrogate modeling and MCS is not exact 8 times compared with the serial one is that there are nine active or violated constraints used to generate the surrogate models while eight cores are used for the parallelization. Therefore, it includes 2 iterations for the parallel computing, 1st iteration for the 1st ~ 8th constraints and 2nd iteration for the 9th constraint only.

Table 5. Comparison of Computational Time

Method	No. of Samples	No. of Constraints	Surrogate Modeling, sec.	MCS, sec.
Parallel	250	9	129.73	337.82
Serial			474.43	1034.79

In this example, the 3rd parallelization explained in Section 4.3, which is the parallelization of FEA, is not used; instead, only one client computer is used for the test. If 50 client computers are used for this test, computer simulation time for the FEA will be almost 50 times faster since the data transmission for the parallelization is negligible. Furthermore, the MPP-based RBDO can use maximally 13 client computers only since there are 13 constraints for the M1A1 Abrams tank roadarm. On the other hand, the sampling-based RBDO can use as many client computers as the number of samples used. The parallelization of FEA is being tested on the U.S. Army TARDEC high performance computing (HPC) system.

6. CONCLUSION

For broader applications, sampling-based RBDO using the DKG method for surrogate model generation and the score function for probability of failure and its sensitivity analysis is proposed in this study. The proposed sampling-based RBDO does not use any approximation on the calculation of the probability of failure and its sensitivity except for

statistical noise due to the MCS, which can be easily solved by increasing the MCS sample set. Furthermore, the proposed method does not use the transformation from the original X-space to the standard normal U-space, which makes performance functions become more highly nonlinear, especially when random inputs are correlated. Therefore, the proposed sampling-based RBDO is more accurate than the sensitivity-based RBDO, which uses approximation and transformation for the probability of failure estimation once surrogate models are sufficiently accurate. The accuracy issue of surrogate models is resolved in this paper by the use of the DKG method. In addition, to enhance the efficiency of the proposed method for high-dimensional problems, the parallel computing is used. Even though only component level RBDO examples are treated in this paper, the proposed sampling-based RBDO can be easily extended to the system-level RBDO by using the failure set of either series or parallel or mixed system. Numerical examples are illustrated to demonstrate how the proposed sampling-based RBDO works compared with the sensitivity-based RBDO. The 2-D mathematical example shows that the proposed method is more accurate and even more efficient than the sensitivity-based RBDO, which means the proposed method is very powerful when the dimension of problems is low. For high-dimensional problems such as the M1A1 Abrams tank roadarm used in the paper, the sampling-based RBDO still yields an accurate optimum design. However, it may require more function evaluation, which can be resolved by parallelizing the computation procedure.

7. ACKNOWLEDGEMENT

This research was primarily supported by the U.S. Army Research Office (Project W911NF-09-1-0250). Some funding for this work was provided by the Automotive Research Center, a U.S. Army Center of Excellence for Modeling and Simulation of Ground Vehicles led by the University of Michigan.

Disclaimer: Reference herein to any specific commercial company, product, process, or service by trade name, trademark, manufacturer, or otherwise, does not necessarily constitute or imply its endorsement, recommendation, or favoring by the United States Government or the Department of the Army (DoA). The opinions of the authors expressed herein do not necessarily state or reflect those of the United States Government or the DoA, and shall not be used for advertising or product endorsement purposes.

8. REFERENCES

1. Chen, X., Hasselman, T.K., and Neill, D. J., "Reliability-Based Structural Design Optimization for

- Practical Applications,” 38th AIAA SDM Conference, AIAA-97-1403, 1997.
2. Wu, Y-T., Shin, Y., Sues, R. H., and Cesare, M. A., “Safety-Factor Based Approach for Probability-Based Design Optimization,” AIAA-2001-1522, 42nd AIAA/ASME/ASC /AHS/ASC SDM Conference & Exhibit, Seattle, Washington, April, 2001.
 3. Du, X., Sudjianto, A., and Chen, W., “An Integrated Framework for Optimization under Uncertainty Using Inverse Reliability Strategy,” ASME Journal of Mechanical Design, Vol.126, No.4, pp. 561-764, 2004.
 4. Zou, T., Mahadevan, S., Sopory, A. “A Reliability-Based Design Method Using Simulation Techniques and Efficient Optimization Approach,” ASME Design Engineering Technical Conferences, Salt Lake City, Utah, DETC2004/DAC-57457, 2004.
 5. Tu, J., and Choi, K.K., “A New Study on Reliability Based Design Optimization,” ASME Journal of Mechanical Design, Vol. 121, No. 4, 1999, pp. 557-564.
 6. Tu, J., Choi, K.K., and Park, Y.H., “Design Potential Method for Robust System Parameter Design,” AIAA Journal, Vol. 39, No. 4, 2001, pp. 667-677.
 7. Choi, K.K., Tu, J., and Park, Y.H., “Extensions of Design Potential Concept for Reliability-Based Design Optimization to Non-Smooth and Extreme Cases,” Journal of Structural and Multidisciplinary Optimization, Vol. 22, No. 5, 2001, pp. 335-350.
 8. Youn, B.D., Choi, K.K., Yang, R-J, Gu, L., “Reliability-Based Design Optimization for Crashworthiness of Vehicle Side Impact,” Journal of Structural and Multidisciplinary Optimization, Vol. 26, No. 3-4, 2004, pp. 272-283.
 9. Youn, B.D., and Choi, K.K., “An Investigation of Nonlinearity of Reliability-Based Design Optimization Approaches,” ASME Journal of Mechanical Design, Vol. 126, 2004, pp. 403-411.
 10. Youn, B.D., and Choi, K.K., “Probabilistic Approaches for Reliability-Based Design Optimization,” AIAA Journal, Vol. 42, No. 1, 2004, pp. 124-131.
 11. Youn, B.D., Choi, K.K., and Park, Y.H., “Hybrid Analysis Method for Reliability-Based Design Optimization,” ASME Journal of Mechanical Design, Vol. 125, No. 2, 2003, pp. 221-232.
 12. Choi, K.K., and Youn, B.D., “Hybrid Analysis Method for Reliability-Based Design Optimization,” 27th ASME Design Automation Conference, September 9-12, 2001, Pittsburgh, PA. Received the 2001 ASME Black and Decker Best Paper Award.
 13. Youn, B.D., Choi, K.K., and Yang, R.J., “Efficient Evaluation Approaches for Probabilistic Constraints in Reliability-Based Design Optimization,” Fifth World Congress of Structural and Multidisciplinary Optimization, May 19-23, 2003, Lido di Jesolo-Venice, Italy. Received the ISSMO-Springer Prize 2003.
 14. Choi, K.K., and Youn, B.D., “An Enriched Performance Measure Approach (PMA+) for Reliability-Based Design Optimization Process,” 2004 SAE World Congress, March 8-11, 2004, Detroit, MI.
 15. Youn, B.D., Choi, K.K., and Du, L., “Enriched Performance Measure Approach (PMA+) and Its Numerical Method for Reliability-Based Design Optimization,” 10th AIAA/ISSMO Multidisciplinary Analysis and Optimization Conference, August 30-September 1, 2004, Albany, NY.
 16. Youn, B.D., and Choi, K.K., “Enriched Performance Measure Approach (PMA+) for Reliability-based Design Optimization,” AIAA Journal, Vol. 43, No. 4, 2005, pp. 874-884.
 17. Yang, R.J., Chuang, C., Gu, L., and Li, G., “Experience with Approximate Reliability-Based Optimization Methods II: An Exhaust System Problem,” Structural and Multidisciplinary Optimization, Vol. 29, No. 6, 2005, pp. 488-497.
 18. Lee, I., Choi, K.K., Du, L., and Gorsich, D., “Dimension Reduction Method for Reliability-Based Robust Design Optimization,” Special Issue of Computer & Structures: Structural and Multidisciplinary Optimization, Vol. 86, 2008, pp. 1550-1562.
 19. Lee, I., Choi, K.K., Du, L., and Gorsich, D., “Inverse Analysis Method Using MPP-based Dimension Reduction for Reliability-Based Design Optimization of Nonlinear and Multi-Dimensional Systems,” Special Issue on Computational Methods in Optimization Considering Uncertainties, Comp. Meth. Appl. Mech. Engrg., Vol. 198, No. 1, 2008, pp. 14-27.
 20. Lee, I., Choi, K.K., and Gorsich, D., “System Reliability-Based Design Optimization Using the MPP-Based Dimension Reduction Method,” Journal of Structural and Multidisciplinary Optimization, Vol. 41, No. 6, 2010, pp. 823-839.
 21. Noh, Y., Choi, K.K., and Du, L., “Reliability-based design optimization of problems with correlated input variables using a Gaussian Copula,” Structural and Multidisciplinary Optimization, Vol. 38, No. 1, 2009, pp. 1-16.
 22. Noh, Y., Choi, K.K., and Lee, I., “Identification of Marginal and Joint CDFs Using the Bayesian Method for RBDO,” Structural and Multidisciplinary Optimization, Vol. 40, No. 1, 2010, pp. 35-51.

23. Noh, Y., Choi, K.K., and Lee, I., "Comparison Study between MCMC-based and Weight-based Bayesian Methods for Identification of Joint Distribution," *Structural and Multidisciplinary Optimization*, Vol. 42, 2010, pp. 823-833.
24. Chang, K.H., Yu, X., and Choi, K.K., "Shape Design Sensitivity Analysis and Optimization for Structural Durability," *Int. J. of Numerical Methods in Engineering*, Vol. 40, 1997, pp. 1719-1743.
25. Grindeanu, I., Choi, K.K., and Chang, K.H., "Shape Design Optimization of Thermoelastic Structures for Durability," *ASME Journal of Mechanical Design*, Vol. 120, No. 3, 1998, pp. 491-500.
26. DRAW Concept Manual, Durability and Reliability Analysis Workspace, Center for Computer-Aided Design, College of Engineering, The University of Iowa, Iowa City, IA, 1994.
27. Yu, X., Chang, K.H., and Choi, K.K., "Probabilistic Structural Durability Prediction," *AIAA Journal*, Vol. 36, No. 4, 1998, pp. 628-637.
28. Youn, B.D., Choi, K.K., and Tang, J., "Structural Durability Design Optimization and Its Reliability Assessment," *International Journal of Product Development*, Vol. 1, Nos. 3/4, 2005, pp. 383-401.
29. Choi, K.K., and Youn, B.D., "Reliability-Based Design Optimization of Structural Durability Under Manufacturing Tolerances," *Fifth World Congress of Structural and Multidisciplinary Optimization*, May 19-23, 2003, Lido di Jesolo-Venice, Italy.
30. Choi, K.K., Youn, B.D., Tang, J., Freeman, J., Stadterman, T., Connon, W., and Peltz, A., "Integrated Computer-Aided Engineering Methodology for Various Uncertainties and Multidisciplinary Applications," *Engineering Design Reliability Handbook*, CRC Press, 2004.
31. Choi, K.K., Tang, J., Hardee, E., and Youn, B.D., "Application of Reliability-Based Design Optimization to Durability of Military Vehicles," 2005 SAE Transactions Journal of Commercial Vehicles, 2005-01-0530.
32. Parametric Technology Corporation, Release 15.0 Pro/ENGINEER Fundamentals, Parametric Technology Corporation, Waltham, MA, 1995.
33. NEiNastran User's Manual Version 9.1, by Noran - NEi Nastran G Noran Engineering, January 2007.
34. CADSI Inc., DADS User's Manual, Rev. 7.5, Oak-dale, IA, 1994.
35. Vanderplaats, G.M., "DOT User's Manual," Version 4.0, VMA Engineering, Goleta, CA 93111, 1993.
36. Stadterman, T., and Mortin, D., "Physics of Failure for Making High Reliability a Reality," Article in *Reliability Edge*, Vol. 4, Issue 2, 2004, pp. 14-15.
37. Choi, K.K., Tang, J., Hardee, E., and Youn, B.D., "Application of Reliability-Based Design Optimization to Durability of Military Vehicles," 2005 SAE Transactions Journal of Commercial Vehicles, 2005-01-0530.
38. Lamb, D.A., Gorsich, D., Krayterman, D., Choi, K.K., Hardee, E., Youn, B.D., and Ghiocel, D., "A Method to Predict the Reliability of Military Ground Vehicles Using High Performance Computing," 25th Army Science Conference, Nov 27-30, 2006, Orlando, FL.
39. Lamb, D., Gorsich, D., Krayterman, D., Choi, K., Hardee, E., Du, L., Youn, B., Bettig, B., and Ghiocel, D., "System Level RBDO for Military Ground Vehicles using High Performance Computing," 2008 SAE World Congress, April 14-18, 2008, Paper #2008-01-0543, Detroit, MI.
40. Lee, I., Choi, K.K., Noh, Y., Zhao, L., and Gorsich, D., "Sampling-Based Stochastic Sensitivity Analysis Using Score Functions for RBDO Problems with Correlated Random Variables," *ASME Journal of Mechanical Design*, Vol.133, 021003, 2011.
41. Lee, I., Choi, K.K., and Zhao, L., "Sampling-Based RBDO Using the Dynamic Kriging Method and Stochastic Sensitivity Analysis," *Structural and Multidisciplinary Optimization*, to appear, 2011.
42. Zhao, L., Choi, K.K., and Lee, I., "A Metamodeling Method Using Dynamic Kriging for Design Optimization," *AIAA Journal*, to appear, 2011.
43. Chiles, J.P., and Delfiner, P., *Geostatistics:-Modeling Spatial Uncertainty*, Wiley, New York, 1999.
44. Martin, J.D. and Simpson, T.W., "Use of Kriging Models to Approximate Deterministic Computer Models," *AIAA Journal*, Vol. 43, No. 4, 2005, pp.853-863.
45. Lewis, R.M., and Torczon, V., "Pattern Search Algorithms for Bound Constrained Minimization," *SIAM Journal on Optimization*, Vol. 9, No. 4, 1999, pp. 1082-1099.
46. Swanson Analysis System Inc., ANSYS Engineering Analysis System User's Manual, Vol. I, II, Houston, PA, 1989.
47. Meggiolaro, M.A., and Castro, J.T.P., "Statistical Evaluation of Strain-Life Fatigue Crack Initiation Predictions," *International Journal of Fatigue*, Vol. 26, No. 5, 2004, pp.463-476.